In Situ Formed Si Nanoparticle Network with Micron-sized Si Particles for Lithium-ion Battery Anodes

Mingyan Wu[1], Julian E.C Sabisch[2], Xiangyun Song[1], Andrew M Minor[2],

Vincent S. Battaglia[1], Gao Liu[1]*

1. Environmental Energy Technologies Division, Lawrence Berkeley National Laboratory, Berkeley, CA 94720. 2. Materials Sciences Division, Lawrence Berkeley National Laboratory, Berkeley, CA 94720, and Department of Materials Science and Engineering, University of California, Berkeley, CA 94704.

ABSTRACT: To address the significant challenges associated with large volume change of micron-sized Si particles as high-capacity anode materials for lithium-ion batteries, we demonstrated a simple but effective strategy: using Si nanoparticles as a structural and conductive additive, with micron-sized Si as the main lithium-ion storage material. The Si nanoparticles connected into the network structure in situ during the charge process, to provide electronic connectivity and structure stability for the electrode. The resulting electrode showed a high specific capacity of 2,500 mAh/g after 30 cycles with high initial coulombic efficiency (73%) and good rate performance during electrochemical lithiation and delithiation: between 0.01 and 1 V vs. Li/Li^+.

KEYWORDS: Silicon, nanoparticle, lithium-ion battery, anode, conductive polymer binder, additives.

To meet the future demands of portable electronics, electric vehicles, and renewable energy storage, tremendous efforts have been devoted to the development of high-performance lithium-ion batteries (LIBs) with high specific energy and long cycle life.[1-5] Silicon (Si) appears to be an attractive candidate for lithium-ion batteries because it delivers 10 times greater theoretical (~4,200 mAh/g) specific capacity than that of a traditional graphite anode (~370 mAh/g).[6, 7] However, the widespread application of silicon materials has remained a significant challenge because of the large volume changes during lithium insertion and extraction processes, particularly when using bulk or micron-sized silicon particles.[8, 9] This large volume change causes cracking and pulverization of silicon, which leads to loss of the electrical contact and drastic capacity fading.[10-12] To address this challenge, various strategies have been explored, and significant progress has been made. Among these efforts, nanostructured Si materials exhibit promising possibilities because of their ability to alleviate mechanical strain induced by volume change.[13] It has been demonstrated that chemically synthesized Si nanostructures, including nanowires,[8, 14] nanocrystals,[15] nanotubes,[16, 17] nanospheres,[18,19] core–shell nanofibers,[20,21] nanoporous materials,[22,23] and Si/carbon nanocomposites[24] showed superior performance compared to bulk Si. However, although mechanical fracture does not take place in Si nanostructures below critical sizes,[15] decreasing particles or grain size is not practical to solve the mechanical instability issue associated with lithium alloy because the movement of Si nanostructures and the detachment from the conducting environment can still be observed due to large volume change during long-term battery cycling.[8, 12, 25-30]

In addition, nanoparticles have huge gravimetric specific surface area, in the range of 50 m^2/g. The volumetric change during lithiation and delithiation creates huge change in active material surface during cycling. Undesirable side reactions due to high surface area at low potential leads

to continued capacity fading in Si nanoparticle-based electrode.[31,32] Other disadvantages, such as low volumetric capacity due to poor packing of nanoparticles, are also of concern. The recent attempt to develop an clamped Si structure that minimizes the contact between the electrolyte and renewing Si surface has led to excellent cycling stability of Si electrode.[50,51]

Micron-sized Si particles have small gravimetric specific surface area, in the range of 0.5 m^2/g, which is advantageous to minimize side reactions induced by surface area changes. The synthesis of micron-sized crystalline Si particles is also more cost effective compared to nanoparticle Si, and therefore easier to scale up for mass manufacture. It has been demonstrated that one way to use micron-sized crystalline Si is to partially convert micron-sized crystalline Si particles to lithiated amorphous Si during initial conditioning cycles and then the two-phase lithiated amorphous/ unlithiated crystalline silicon structure was maintained by cycling them with a lower voltage limit in the following cycles .[33] Zhang and his co-workers used a two-step process to convert micrometer porous Si to chemical vapor deposition (CVD)-coated Si surface and pores, then used conductive, chain-like feature of Ketjenblack (KB) carbon additives to maintain the conductivity.[34] Cui and his co-workers used interconnected micron-sized silicon hollow nanospheres as LIB anodes and observed long cycle life (700 cycles) with high specific capacity (2725 mAh/g).[19]The same group also used amorphous silicon as an inorganic glue to replace the conventional polymer binder, which enabled both nano- and micron-sized silicon to be stably cycled over 200 cycles with 800 mAh/g capacity.[46]However, both methods involved CVD steps at high temperature.

Another strategy is to take advantages of both materials by the combination of nano- and micron-sized materials. Several approaches have been developed: encapsulating nanomaterials with the microshell,[31,35] coating a nanosized layer on micron-sized materials,[36] and growing 1D nanowires on the surface of micron-sized active materials.[37-39]

In addition, there is now recognition of the critical role of the polymer binders in maintaining the structure for Si electrodes and thereby enabling them to achieve repeatable LIB operation.[47-49] We recently developed conductive polymer binders which showed good electrochemical

performance when used in an Si nanoparticle-based anode for LIBs.[40,45] However, when one type of this polymer binder Poly(9,9-dioctylfluorene-co-fluorenone-co-methylbenzoic ester) (PFM) was applied to micron-sized Si particles, fast fading was still observed due to the mechanical degradation of the Si electrode during cycling. Similarly, this has been demonstrated when using the conventional polymer binder PVDF in prior works. Herein we report a new strategy: by simply adding small amount of nanosized Si (n-Si) as an additive, along with the advantages of the conductive polymer binder, we are able to apply low-cost and low-specific-area micron-sized silicon particles (m-Si) into lithium-ion battery anodes with high specific capacity and significantly improved cycle life.

This system offers three advantages over conventional pure micron-sized silicon-, AB-, and PVDF-based electrodes: (1) The in situ formed n-Si and m-Si 3D network takes advantage of the high surface area of small-sized n-Si, thereby significantly alleviating the huge stress created by m-Si during the lithiation and delithiation process. It has been proven that small enough materials can relax the stress and therefore help to overcome pulverization.[8, 12, 13, 15, 25-30] (2) This network works like three-dimensional cross-linked advanced polymer binders, which have been shown in literature to help confine the Si particles in place, with higher resistance to strain - particularly non-recoverable deformation.[49] (3) Using a novel conductive polymer binder PFM over the insulating PVDF to replace the nonbonding acetylene black is another advantage of this system. [40] All these three aspects play an indispensable role in this system's success.

During the first lithiation process, both m-Si and n-Si particles become a lithiated alloy, soften, and expand in size. The mechanical compression between the lithiated Si particles causes the softened particles to touch and eventually connect covalently into a nanosized-network structure around the m-Si particles. The network structure can prevent further compression of the electrode and retain the conductive polymer binders around the m-Si particles. This structure feature also allows the mechanical strain induced by volume change from m-Si to relax,

therefore preventing severe electrode breakdown and fast capacity fading (Fig. 1). Figure 1a shows the schematic presentation of composite anode electrode using m-Si, the conductive polymer binder PFM and conductive additive acetylene black (AB). AB is nanosized conductive additive used in lithium-ion batteries since its early days.[41] While AB is used in the electrode, it does not contribute to energy storage and acts as a "passive" conductivity enhancer to facilitate electron transport from the active materials to the current collector, which improves electrode power capability. However, because AB has no mechanical binding force to either the Si or the conductive polymer binder PFM, during the large volume expansion of any individual m-Si particles (which is in cube micrometer range) both AB and polymer binders tend to be pushed away from the m-Si particles, leading to a void space or gap between the m-Si particles and the conductive network, leading to broken electrical connections. To maintain conductivity and power capability, a relatively large amount of AB needs to be added, which reduces the volumetric and gravimetric lithium-ion storage capacity.[2,11] In contrast, when AB is replaced with n-Si particles, as shown in Fig. 1b, n-Si tends to self-assemble on the surface of m-Si and form a new 3D network structure with m-Si during the lithiation process. This network forms physical connections between m-Si and helps to draw polymer binder back and holding the integrity of the electrodes during the large volume extraction process of delithiation. To the best of our knowledge, such a strategy has not been reported for m-Si in lithium-ion batteries before, and its facile and scalable features would benefit the research community, which is focusing on high-performance lithium-ion batteries with high specific energy and long cycle life at low cost.

It has been known that m-Si-based lithium-ion batteries fail in a few cycles due to the pulverization and fatigue of the electrode arising from stresses generated by the huge volume change of Si associated with the insertion and extraction of lithium.[22] Similar results of composited electrode m-Si/AB/PFM were obtained, as shown in Fig. 2a. The anode was composited of 50% 4.6 μm of m-Si, 20% AB, and 30% PFM in mass ratio. Lithium was used as counter electrode. The mass loading for only m-Si was about 0.16 mg/cm^2, and m-Si/n-Si was 0.23 mg/cm^2. Other submicron- or micron-sized Si, including 200–400 nm and 0.8 μm Si under

different mass ratio, were also tested and showed similar improved performance under this optimized composition.(see Fig. S1 a–f in supplemental information for more details) As shown in Fig.2a, cycling of m-Si/AB/PFM started at high lithiation capacity but faded quickly to nearly 0 within five cycles, with large initial irreversible capacity. In contrast, as n-Si replaced AB (Fig. 2b), a high discharge capacity with only a small decrease was observed within five cycles with a high initial coulombic efficiency of 73%. More significantly, the charge capacity retention was kept up to 75% over 30 cycles.

To explore the mechanism behind the superior performance of n-Si when replacing AB, we dissembled cells after five cycles for each composition and rinsed the electrodes with EC/DEC 1:1 and DMC solvents, respectively, then washed them with chloroform. In this way, the dissolvable polymer binder, the residue electrolyte, and most of the soluble form of the SEI layer were washed away and the rest of the structure components, such as Si and AB, were kept.

Fig. 3a shows the pristine m-Si SEM image, and Figs. 3b and 3c show SEM images of fresh m-Si/AB/PFM and m-Si/n-Si/PFM electrodes before cycling, respectively. Fig. 3d shows the m-Si/AB/PFM electrode after five cycles of charge/discharge, and washed as described above. Isolated m-Si particles with no physical connections to the electrode were observed in the electrode, similar to the pristine m-Si SEM image (Fig. 3a). However, when the AB was replaced with n-Si, the m-Si exhibited a fluffy structure which was formed by in situ-connected n-Si particles on its surface (Figs. 3e, 3f, 3h).

Li and his co-workers observed the distorted and destroyed Si bonds in Si nanowires during lithium insertion, but when the lithium was extracted by same method from Si nanowires, some distorted and interrupted bonds will be rebonded, so a local, ordered structure formed in the Li-doped Si nanowires.[42] They demonstrated that when the distance between neighboring Si columns is close enough in a double-pattern microcolumn electrode, each Si column is expanded and merge together to form new regular hole-like patterns during lithium insertion and extraction.[43] Therefore, the fluffy network structure of m-Si/n-Si is most likely the new Si-Si

structure, due to the formation of bonds between m-Si particles and n-Si particles. To further verify this proposed new structure, focused ion beam (FIB) experiments were carried out in an FEI Quanta 3D FEG 200/600 model microscope containing both scanning electron microscope (SEM) and focused ion beam (FIB). The sample was sputtered with ~100 nm gold film then deposited upon carbon tape by pressing the m-Si containing substrate onto a piece of carbon film. A typical particle was chosen for investigation and the appropriate beam current was applied to cut it in half, to show the cross section (see Experimental details in Supporting Information and Fig. 3g). As in Fig. 3g, the main particle was the host m-Si, and n-Si was strongly bonded to the m-Si surface, as can be seen in the cross section of this structure. In addition, minor cracks in the m-Si can also be observed, due to volume expansion after cycles, but the main shape was well maintained (see Fig. S2a, b for different magnification and vision angle).

Nanosized alloy particles tend to agglomerate together during electrochemical cycling. This was explained by decreasing the high surface energy of the nanoparticles. It has also been shown that the agglomerate occurs in both n-Si and m-Si particles and that serious irreversible agglomeration is not favorable to achieving good capacity retention.[43,44] Adding n-Si particles into m-Si based electrodes as additives helps to prevent a severe agglomeration of m-Si particles due to in situ connected n-Si particles on their surface. The in situ-formed network structure significantly releases the stress induced by large volume change of the m-Si during the lithium insertion/extraction process. The electrode composited by this network will retain higher porosity compared to a pure m-Si electrode, due to self-assembled n-Si on m-Si, and therefore enhance the cycle stability and rate capacity dramatically.

The rate performance of m-Si/n-Si/PFM composite electrodes were also tested, as shown in Fig. 4. Over 80% of capacity was maintained at a 1C charge rate, and only about a 100 mV higher average discharge potential than that of the C/25 discharge rate was observed. This further confirmed that the delithiation of the Li and Si alloy is a facile process, and that it can support a high rate of discharge of Si anode-based batteries.

In summary, we described a facile but effective strategy utilizing micron-sized silicon materials as anodes for lithium-ion batteries. By simply adding nanosized silicon into micron-sized silicon particles, n-Si tends to self-assemble on the surface of m-Si and form a conductive 3D network during battery operation. The resulting composite electrode showed a significantly improved electrochemical performance, including a highly reversible Li storage capacity, good cycling performance, good rate performance, and high initial coulombic efficiency. The entire fabrication process is scalable and does not involve expensive silicon growth steps.

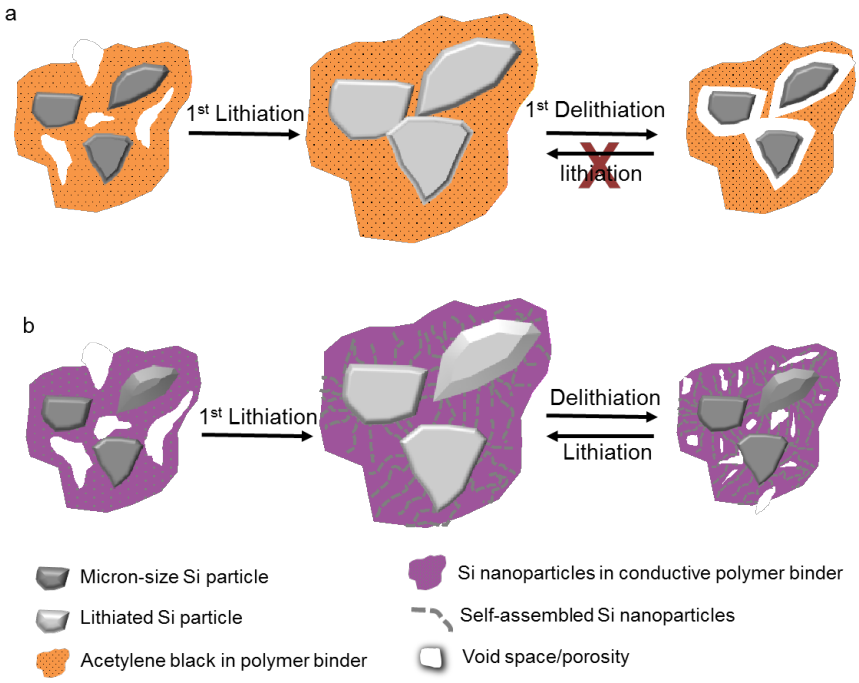

Figure 1. Schematics of lithiation and delithiation process of composite anode electrodes using micron-sized Si particles as active lithium-ion storage materials. (a) When an acetylene black conductive additive is used, the absolute volume expansion of any individual particles is in cube micrometer range. This large volume change has pushed the binders and AB composite to expand during charge. During discharge, the AB/binder composite does not fully recover, leaving gaps between the Si active materials and the AB/binder conductive matrix. (b) When Si nanoparticles are used as an additive along with a conductive polymer binder during the charge

process, the Si nanoparticles and micron-sized Si tend to fuse to form a network structure to cushion the volume expansion. The physical connections between the micron-sized Si particles and the conductive network are preserved during the discharge process.

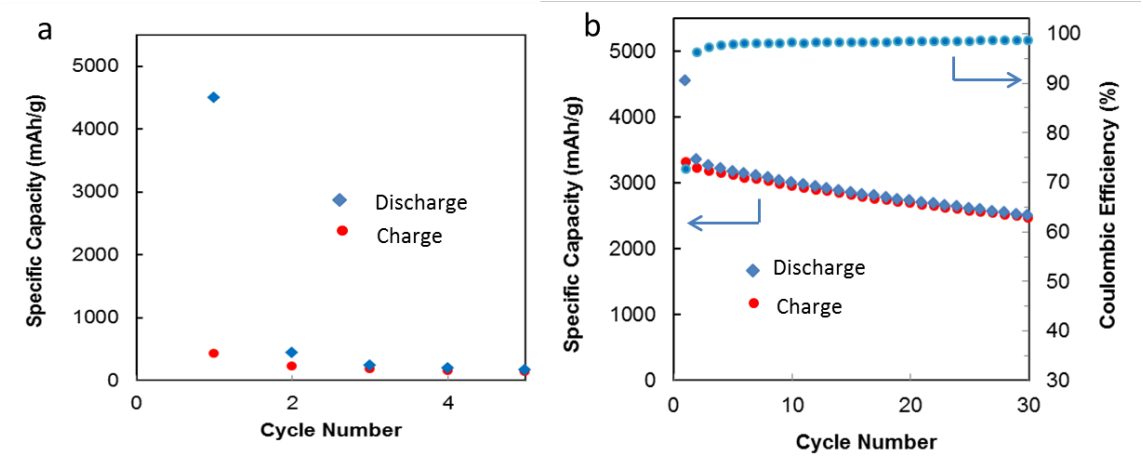

Figure 2. Electrochemical performance of composite electrodes (a) m-Si/AB/PFM, (b) m-Si/n-Si/PFM

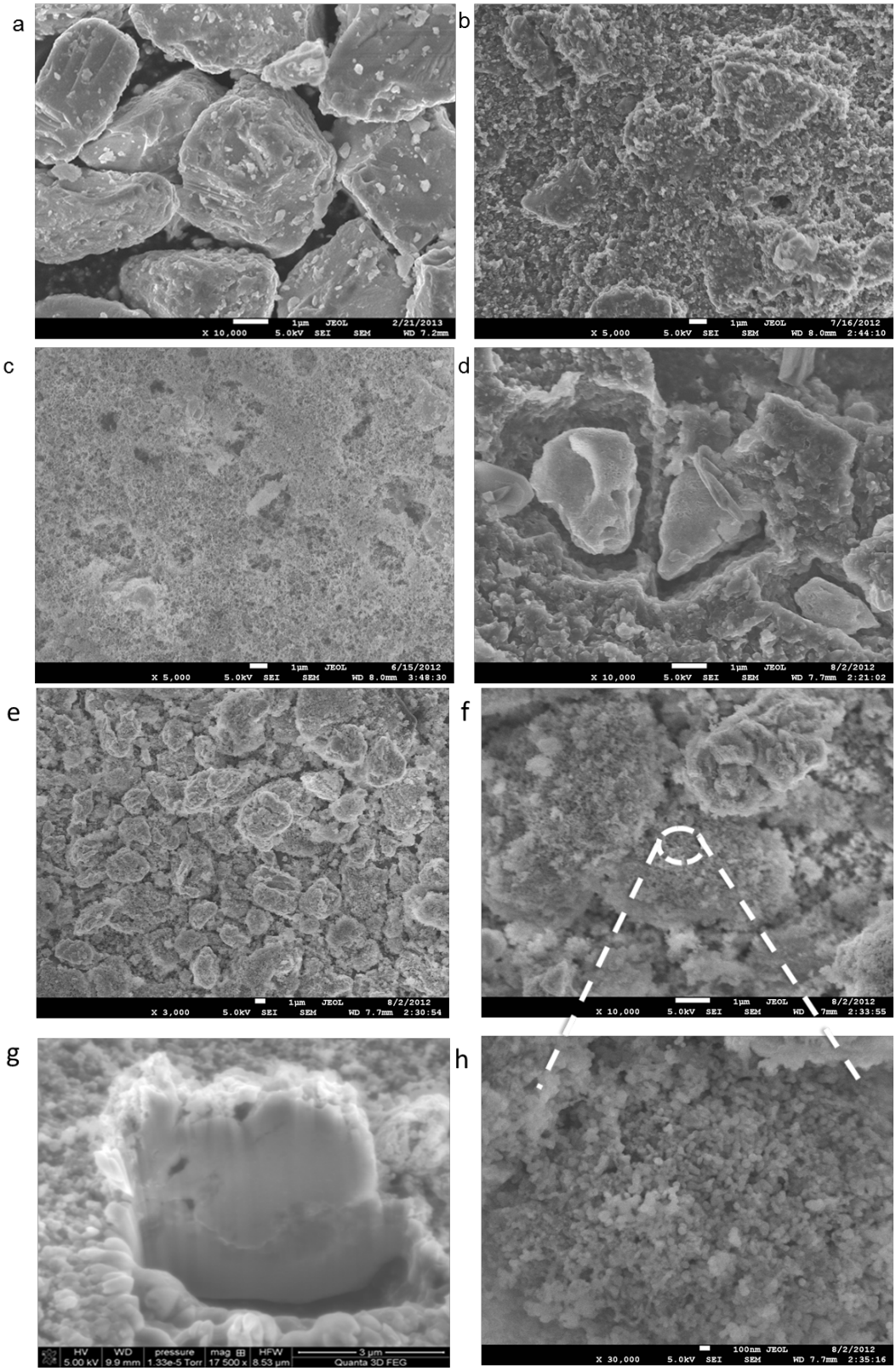
a
b
c
d
e
f
g
h
1µm JEOL 2/21/2013
X 10,000 5.0kV SEI SEM WD 7.2mm
1µm JEOL 7/16/2012
X 5,000 5.0kV SEI SEM WD 8.0mm 2:44:10
1µm JEOL 6/15/2012
X 5,000 5.0kV SEI SEM WD 8.0mm 3:48:30
1µm JEOL 8/2/2012
X 10,000 5.0kV SEI SEM WD 7.7mm 2:21:02
1µm JEOL 8/2/2012
X 3,000 5.0kV SEI SEM WD 7.7mm 2:30:54
1µm JEOL 8/2/2012
X 10,000 5.0kV SEI SEM WD 7mm 2:33:55
HV WD pressure mag HFW
5.00 kV 9.9 mm 1.33e-5 Torr 17 500 x 8.53 µm
3 µm
Quanta 3D FEG
100nm JEOL 8/2/2012
X 30,000 5.0kV SEI SEM WD 7.7mm 2:35:16

Figure 3. Representative SEM images of: (a) the pristine m-Si particles, (b) fresh m-Si/AB/PFM electrode, (c) fresh m-Si/n-Si/PFM electrode, (d) the electrode of m-Si/AB/PFM after 5 cycles and wash, (e) lower magnification of the electrode of m-Si/n-Si/PFM after 5 cycles and wash, (f) middle magnification of the electrode of m-Si/n-Si/PFM after 5 cycles and wash, (g) FIB cross-section image of a cycled m-Si particles with Si nanoparticles firmly attached on the surface, and (h), higher magnification of the electrode of m-Si/n-Si/PFM after 5 cycles and wash.

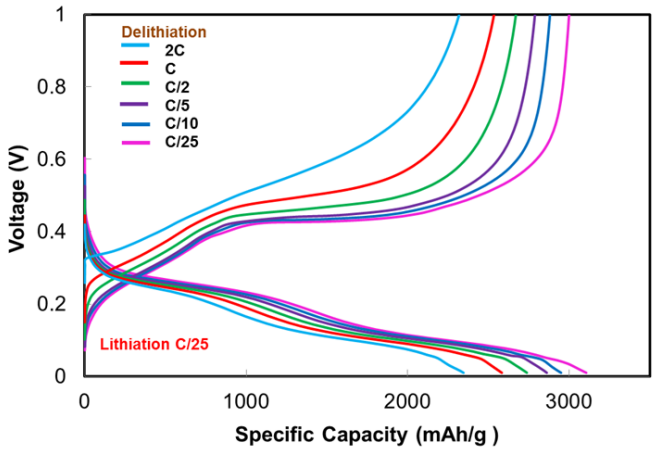

Figure 4. Rate performance of composite electrode m-Si/n-Si/PFM

Supporting Information. Experimental details. Polymer binder synthesis, electrode casting, cell fabrication and testing, cycle performance of different sizes of m-Si with different mass ratio to n-Si and PFM, SEM measurement, FIB experiments. This material is available free of charge via the Internet at http://pubs.acs.org.

AUTHOR INFORMATION

Corresponding Author

*E-mail: gliu@lbl.gov

ACKNOWLEDGMENTS

This work is funded by the Assistant Secretary for Energy Efficiency, Office of Vehicle Technologies of the U.S. Department of Energy, under the Batteries for Advanced Transportation Technologies (BATT) Program and by University of California, Office of the President through the University of California Discovery Grant. Electron microscopy experiments were conducted at the National Center for Electron Microscopy (NCEM), located at Lawrence Berkeley National Laboratory (LBNL) and supported by the Director, Office of Science, Office of Basic Energy Sciences, of the U.S. Department of Energy under contract no. DE-AC02-05CH11231.

REFERENCES

(1) Armand, M.; Tarascon, J. M. *Nature* **2008,** *451*, 652-657.
(2) Kang, B.; Ceder, G. *Nature* **2009,** *458*, 190-193.
(3) Tarascon, J. M.; Armand, M. *Nature* **2001,** *414*, 359-367.
(4) Bruce, P. G.; Scrosati, B.; Tarascon, J. M. *Angew. Chem. Int. Edit.* **2008,** *47*, 2930-2946.
(5) Whittingham, M. S. *Mrs. Bull.* **2008,** *33*, 411-419.
(6) Boukamp, B. A.; Lesh, G. C.; Huggins, R. A. *J. Electrochem. Soc.* **1981,** *128*, 725-729.
(7) Li, J.; Dahn, J. R. *J. Electrochem. Soc.* **2007,** *154*, A156-A161.
(8) Chan, C. K.; Peng, H. L.; Liu, G.; McIlwrath, K.; Zhang, X. F.; Huggins, R. A.; Cui, Y. *Nature Nanotechnology* **2008,** *3*, 31-35.
(9) Hatchard, T. D.; Dahn, J. R. *J. Electrochem. Soc.* **2004,** *151*, A838-A842.
(10) Christensen, J.; Newman, J. *J. Electrochem. Soc.* **2006,** *153*, A1019-A1030.
(11) Renganathan, S.; Sikha, G.; Santhanagopalan, S.; White, R. E. *J. Electrochem. Soc.* **2010,** *157*, A155-A163.
(12) Ryu, J. H.; Kim, J. W.; Sung, Y. E.; Oh, S. M. *Electrochem. Solid St* **2004,** *7*, A306-A309.
(13) Wu, H.; Zheng, G. Y.; Liu, N. A.; Carney, T. J.; Yang, Y.; Cui, Y. *Nano Lett.* **2012,** *12*, 904-909.
(14) Huang, R.; Fan, X.; Shen, W. C.; Zhu, J. *Appl. Phys. Lett.* **2009,** *95*.
(15) Kim, H.; Seo, M.; Park, M. H.; Cho, J. *Angew. Chem. Int. Edit.* **2010,** *49*, 2146-2149.
(16) Park, M. H.; Kim, M. G.; Joo, J.; Kim, K.; Kim, J.; Ahn, S.; Cui, Y.; Cho, J. *Nano Lett.* **2009,** *9*, 3844-3847.
(17) Song, T.; Xia, J. L.; Lee, J. H.; Lee, D. H.; Kwon, M. S.; Choi, J. M.; Wu, J.; Doo, S. K.; Chang, H.; Il Park, W.; Zang, D. S.; Kim, H.; Huang, Y. G.; Hwang, K. C.; Rogers, J. A.; Paik, U. *Nano Lett.* **2010,** *10*, 1710-1716.
(18) Ma, H.; Cheng, F. Y.; Chen, J.; Zhao, J. Z.; Li, C. S.; Tao, Z. L.; Liang, J. *Adv. Mater.* **2007,** *19*, 4067-4070.
(19) Yao, Y.; McDowell, M. T.; Ryu, I.; Wu, H.; Liu, N. A.; Hu, L. B.; Nix, W. D.; Cui, Y. *Nano Lett.* **2011,** *11*, 2949-2954.
(20) Cui, L. F.; Ruffo, R.; Chan, C. K.; Peng, H. L.; Cui, Y. *Nano Lett.* **2009,** *9*, 491-495.
(21) Cui, L. F.; Yang, Y.; Hsu, C. M.; Cui, Y. *Nano Lett.* **2009,** *9*, 3370-3374.
(22) Teki, R.; Datta, M. K.; Krishnan, R.; Parker, T. C.; Lu, T. M.; Kumta, P. N.; Koratkar, N. *Small* **2009,** *5*, 2236-2242.
(23) Kim, H.; Han, B.; Choo, J.; Cho, J. *Angew. Chem. Int. Edit.* **2008,** *47*, 10151-10154.
(24) Magasinski, A.; Dixon, P.; Hertzberg, B.; Kvit, A.; Ayala, J.; Yushin, G. *Nature Materials* **2010,** *9*, 353-358.
(25) Park, C. M.; Kim, J. H.; Kim, H.; Sohn, H. J. *Chem. Soc. Rev.* **2010,** *39*, 3115-3141.
(26) Choi, N. S.; Yao, Y.; Cui, Y.; Cho, J. *J. Mater. Chem.* **2011,** *21*, 9825-9840.
(27) Hertzberg, B.; Alexeev, A.; Yushin, G. *J. Am. Chem. Soc.* **2010,** *132*, 8548-8549.
(28) Kamali, A. R.; Fray, D. J. *J. New Mat. Electr. Sys* **2010,** *13*, 147-160.
(29) Beaulieu, L. Y.; Eberman, K. W.; Turner, R. L.; Krause, L. J.; Dahn, J. R. *Electrochem. Solid St* **2001,** *4*, A137-A140.
(30) Chan, C. K.; Ruffo, R.; Hong, S. S.; Cui, Y. *J. Power Sources* **2009,** *189*, 1132-1140.
(31) Guo, Y. G.; Hu, J. S.; Wan, L. J. *Adv. Mater.* **2008,** *20*, 2878-2887.
(32) Liu, C.; Li, F.; Ma, L. P.; Cheng, H. M. *Adv. Mater.* **2010,** *22*, E28-E62.
(33) Obrovac, M. N.; Krause, L. J. *J. Electrochem. Soc.* **2007,** *154*, A103-A108.
(34) Xiao, J.; Xu, W.; Wang, D. Y.; Choi, D. W.; Wang, W.; Li, X. L.; Graff, G. L.; Liu, J.; Zhang, J. G. *J. Electrochem. Soc.* **2010,** *157*, A1047-A1051.
(35) Deng, D.; Lee, J. Y. *Chem. Mater.* **2008,** *20*, 1841-1846.
(36) Hu, Y. S.; Guo, Y. G.; Dominko, R.; Gaberscek, M.; Jamnik, J.; Maier, J. *Adv. Mater.* **2007,** *19*, 1963-1966.
(37) Zhang, Y.; Zhang, X. G.; Zhang, H. L.; Zhao, Z. G.; Li, F.; Liu, C.; Cheng, H. M. *Electrochim. Acta* **2006,** *51*, 4994-5000.

(38) Chen, J.; Minett, A. I.; Liu, Y.; Lynam, C.; Sherrell, P.; Wang, C.; Wallace, G. G. *Adv. Mater*. **2008,** *20*, 566-570.
(39) Zhang, H. L.; Zhang, Y.; Zhang, X. G.; Li, F.; Liu, C.; Tan, J.; Cheng, H. M. *Carbon* **2006,** *44*, 2778-2784.
(40) Liu, G.; Xun, S. D.; Vukmirovic, N.; Song, X. Y.; Olalde-Velasco, P.; Zheng, H. H.; Battaglia, V. S.; Wang, L. W.; Yang, W. L. *Adv. Mater*. **2011,** *23*, 4679-4683.
(41) Chen, Y. H.; Wang, C. W.; Liu, G.; Song, X. Y.; Battaglia, V. S.; Sastry, A. M. *J. Electrochem. Soc*. **2007,** *154*, A978-A986.
(42) Zhou, G. W.; Li, H.; Sun, H. P.; Yu, D. P.; Wang, Y. Q.; Huang, X. J.; Chen, L. Q.; Zhang, Z. *Appl. Phys. Lett*. **1999,** *75*, 2447-2449.
(43) He, Y.; Yu, X. Q.; Li, G.; Wang, R.; Li, H.; Wang, Y. L.; Gao, H. J.; Huang, X. J. *J. Power Sources* **2012,** *216*, 131-138.
(44) Li, H.; Shi, L. H.; Wang, Q.; Chen, L. Q.; Huang, X. J. *Solid State Ionics* **2002,** *148*, 247-258.
(45) Wu, M.; Xiao, X.; Vukmirovic, N.; Xun, S.; Kumar Das , P.; Song, X.; Olalde-Velasco, P.; Wang, D.; Weber, A. Z.; Wang, L.; Battaglia, V. S.; Yang, W.; and Liu, G. *J. Am. Chem. Soc*.**2013**, just accepted, **DOI:** 10.1021/ja4054465
(46) Cui, L.; Hu, L.; Wu, H.; Choi, J.; and Cui, Y. *J. Electrochem. Soc.* **2011** *158*, A592-A596
(47) Ryou, M. H.; Kim, J.; Lee, I.; Kim, S.; Jeong, Y. K.; Hong, S.; Ryu, J. H.; Kim, T. S.; Park, J. K.; Lee, H.; Choi, J. W. *Adv. Mater.* **2013**, *25*, 1571-1576
(48) Kovalenko, I.; Zdyrko, B.; Magasinski, A.; Hertzberg, B.; Milicev, Z.; Burtovyy, R.; Luzinov, I.; Yushin, G. *Science* **2011**, *334*, 75-79
(49) Koo, B.; Kim, H.; Cho, Y.; Lee, K. T.; Choi, N. S.; Cho, J. *Angew Chem Int Edit.* **2012**, *51*, 8762-8767
(50) Liu, N.;, Wu, H.; McDowell, M. T.; Yao, Y.; Wang, C.; Cui, Y. *Nano Lett.*, 2012, *12*, 3315–3321
(51) Wu, H.; Chan, G.; Choi, J. W.; Ryu, I.; Yao, Y.; Mcdowell, M. T.; Lee, S. W.; Jackson, A.; Yang, Y.; Hu, L.; Cui, Y. *Nature Nanotech*., **2012**, *7*, 310-315